Bioconjugate Chemistry

Article

pubs.acs.org/bc

Hyaluronic Acid-Based Nanogel–Drug Conjugates with Enhanced Anticancer Activity Designed for the Targeting of CD44-Positive and Drug-Resistant Tumors

Xin Wei, Thulani H. Senanayake, Galya Warren, and Serguei V. Vinogradov*

Center for Drug Delivery and Nanomedicine and Department of Pharmaceutical Sciences, College of Pharmacy, University of Nebraska Medical Center, Omaha, Nebraska 68198-6025, United States

Supporting Information

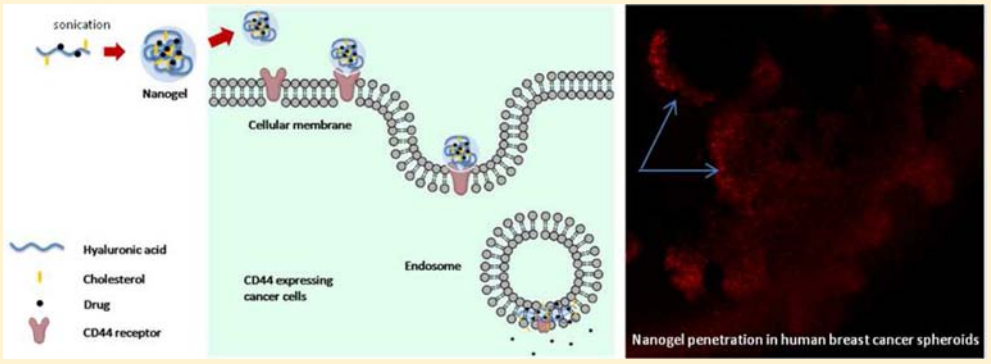

ABSTRACT: Many drug-resistant tumors and cancer stem cells (CSC) express elevated levels of CD44 receptor, a cellular glycoprotein binding hyaluronic acid (HA). Here, we report the synthesis of nanogel–drug conjugates based on membranotropic cholesteryl-HA (CHA) for efficient targeting and suppression of drug-resistant tumors. These conjugates significantly increased the bioavailability of poorly soluble drugs with previously reported activity against CSC, such as etoposide, salinomycin, and curcumin. The small nanogel particles (diameter 20–40 nm) with a hydrophobic core and high drug loads (up to 20%) formed after ultrasonication and demonstrated a sustained drug release following the hydrolysis of biodegradable ester linkage. Importantly, CHA–drug nanogels demonstrated 2–7 times higher cytotoxicity in CD44-expressing drug-resistant human breast and pancreatic adenocarcinoma cells compared to that of free drugs and nonmodified HA–drug conjugates. These nanogels were efficiently internalized via CD44 receptor-mediated endocytosis and simultaneous interaction with the cancer cell membrane. Anchoring by cholesterol moieties in the cellular membrane after nanogel unfolding evidently caused more efficient drug accumulation in cancer cells compared to that in nonmodified HA–drug conjugates. CHA–drug nanogels were able to penetrate multicellular cancer spheroids and displayed a higher cytotoxic effect in the system modeling tumor environment than both free drugs and HA–drug conjugates. In conclusion, the proposed design of nanogel–drug conjugates allowed us to significantly enhance drug bioavailability, cancer cell targeting, and the treatment efficacy against drug-resistant cancer cells and multicellular spheroids.

INTRODUCTION

The most current therapeutic strategies are unable to completely eliminate tumors and to overcome the emerging resistance to many anticancer drugs and tumor relapse, providing only palliative solutions to cancer patients. The development of drug resistance and tumor relapse have been closely associated recently with the accumulation of cancer-initiating or cancer stem cells (CSCs) in tumors following chemotherapy.[1] These CSCs are characterized by over-expression of drug efflux transporters, formation of multicellular spheroids, and overall reduced metabolic activity, which make them resistant to cytotoxic drugs.[2] Drug combination therapies, immunotherapies, and nanoformulated drugs were found effective in order to circumvent the drug resistance.[3] Nano-delivery can also improve the solubility of many low soluble drugs, increase drug accumulation in tumors, and decrease cytotoxic side effects. Although, significant progress was made in the development of nanodelivery, even the most advanced drug delivery systems such as liposomes and polymer micelles are far from optimal; for example, encapsulated drugs can rapidly diffuse through the liposome bilayer, while micellar drugs often demonstrated *in vivo* instability, and both systems sometimes had drug loading capacity too low to produce a therapeutic effect.[4,5] Prodrug approaches using polymeric drug conjugates look more attractive because of the higher drug loading capacity and controlled drug release depending on the

Received: November 26, 2012
Revised: March 21, 2013
Published: April 2, 2013

dx.doi.org/10.1021/bc300632w | *Bioconjugate Chem.* 2013, 24, 658–668

drug-linker stability.[6] We recently reported the synthesis of cholesteryl nanogel−drug conjugates that contained biodegradable tetraphosphate linkers and could deliver cytotoxic nucleoside analogues in activated phosphorylated form.[7] These polyvinyl alcohol or dextrin-based nanogel−drug conjugates demonstrated excellent activity against many resistant to nucleoside analogue cancer cells. In this article, we extend this successful nanogel design to the preparation of biodegradable hyaluronic acid−drug conjugates that could be applied to the treatment of CD44-positive drug-resistant cancer cells and, potentially, CSCs.

Hyaluronic acid (HA) is a linear anionic polymer composed of repeating disaccharide unites of β-1,4-D-glucuronic acid-β-1,3-*N*-acetyl-D-glucosamine. HA with different MWs play different roles in the body. Low-MW polymers typically induce receptor-mediated intracellular signaling, while high MW-polymers maintain cell integrity and matrix organization.[8] This biocompatible, biodegradable, and nonimmunogenic biomaterial has been extensively studied in pharmaceutical and biomedical applications, including cancer therapy, when various drugs have been conjugated to HA, like paclitaxel or doxorubicin.[9−11] Many drug-resistant cancer cells and CSCs display elevated levels of CD44 receptors that bind HA.[12] Potentially, CD44 can be targeted for the treatment of drug-resistant tumors and CSCs.[34] Previously, it was shown that HA-grafted liposomes have an increased cellular uptake through CD44-mediated endocytosis, which is a highly regulated process of binding, internalization, and ligand transfer through a series of intracellular compartments.[13,14]

Hydrophobic modification of polymer prodrugs can improve the internalization of nanocarriers through interaction with the cellular membrane. Modification with cholesterol, which is a common component of the cellular membrane, resulted in significant improvement of the cellular accumulation of various macromolecules (e.g., siRNA) and polymers for drug delivery applications.[18,19] The presence of hydrophobic moieties was also helpful in the preparation of compact polymeric nanoparticles or nanogels after ultrasonication of modified polymers in water. For example, nanoparticles formed from ceramide-modified HA (HACE) have been recently introduced as drug carriers and bioimaging probes.[15−17] Here, our goal was to assemble nanocarriers, which could deliver drugs more efficiently than simple HA−drug conjugates, and apply them to the treatment of drug-resistant cancer cells, spheroids and, potentially, CSC. For this purpose, we designed and evaluated novel compact nanogels based on cholesterol-modified HA (CHA) that could be conjugated via biodegradable covalent linkage with selected drugs previously found to be highly active against CSCs.

A high throughput drug screening study identified several drug candidates for the treatment of CSCs, like etoposide (ETO) and salinomycin (SAL).[20] Salinomycin, a veterinary antibiotic, displayed 100 times higher efficacy against CSCs than paclitaxel. The major shortcoming of salinomycin was its toxicity, which did not allow the application of the drug to human patients. Etoposide, a topoisomerase inhibitor and popular anticancer drug, was only a little less active than salinomycin. The toxicity profile of etoposide as an anticancer drug was far from optimal, demonstrating hematologic and gastrointestinal toxicity. The novel potential anticancer drug, curcumin (CUR), demonstrated efficacy against multiple cancer targets and was also found very effective against CSCs.[21] However, low stability and poor bioavailability of curcumin reduce its value as a drug.

Here, we designed nanogel−drug conjugates that are free of many of these shortcomings. All these drugs (ETO, SAL, and CUR) contain hydroxyl groups in their chemical structure, which form biodegradable esters after chemical conjugation with carboxyl groups of HA. The CHA−drug conjugates form compact stable nanogels due to the intramolecular folding of HA strands and the formation of the hydrophobic core after ultrasonication in aqueous solution. These nanogels could effectively target CD44 receptors on drug-resistant cancer cells. Evidently, these nanogels could unfold on cellular membrane anchoring in the lipid bilayer by multiple cholesterol moieties. This process may lead to the formation of semipermeable patches in the cellular membrane and results in efficient cytoplasmic drug release and the eventual inhibition of cancer cell growth.

MATERIALS AND METHODS

Materials. Most reagents and solvents were purchased from Sigma-Aldrich (St. Louis, MO) unless otherwise indicated. 5-Fluoro-2′-deoxyuridine (Floxuridine, FdU) was from SynQuest Laboratories (Alachua, FL). Dialysis tubing (MWCO, 12−14 kDa) was purchased from Fisher Scientific (Pittsburgh, PA). The silicagel for column chromatography was from Whatman (GE Healthcare, USA). Etoposide was purchased from Ochem (Des Plaines, IL). Salinomycin was purchased from Chemieliva Pharmaceutical (Chongqing, China). Hyaluronic acid sodium salt (MW 62 kDa) was purchased from Quingao Biomedical (Chaska, China).

Cell Lines. Human breast carcinoma cell lines MDA-MB-231 and MCF-7 were obtained from ATCC (Rockville, MD). Human pancreatic cancer MIA PaCa-2 cells were a kind gift from Dr. Surinder K. Batra (Eppley Cancer Institute, UNMC). MCF-7 and MIA PaCa-2 cells were maintained in Dulbecco's modified Eagle's medium (DMEM, HyClone/ThermoScientific) supplemented with 10% fetal bovine serum (FBS), 1% L-glutamate, and 2% penicillin/streptomycin. MDA-MB-231 cells were grown in DMEM/Nutrient mixture F-12 (DMEM/F12, HyClone/ThermoScientific) with the same additives. Drug-resistant MDA-MB-231/F cells were selected by routine exposure to the increasing doses of floxuridine over the period of 6 months. The resistant cell line was cultured in the same growth medium containing 10 μg/mL floxuridine to maintain the drug-resistant phenotype. All cells were cultured at 37 °C in humidified atmosphere with 5% CO_2.

Synthesis of Cholesteryl-Hyaluronic Acid (CHA). Aqueous solution of HA (sodium salt) was passed through a column with Dowex 50 × 8 (H^+-form) and lyophilized. A solution of 2,2′-(ethylenedioxy)-bis-ethylamine linker (L) (5 g, 30 mmol) in 30 mL of anhydrous dichloromethane (DCM) containing 0.75 g (7.5 mmol) of triethylamine was used in reaction with cholesteryl chloroformate (CC) (3.36 g, 7.5 mmol) dissolved in 20 mL of DCM and added dropwise over 30 min under argon. The final mixture was stirred overnight at 25 °C, filtered, and concentrated *in vacuo*. The cholesteryl-amine linker was isolated following column chromatography on silica gel using a stepwise methanol gradient (6, 9, 12 and 15%) in DCM with a yield of 76%.

Cholesteryl-HA (CHA) was synthesized by activation of HA (4 g, 10 mmol carboxyl groups), dried by coevaporation with toluene *in vacuo*, and dissolved in 100 mL of warm anhydrous dimethyl sulfoxide (DMSO) using 100 mg (0.64 mmol) of 1-

dx.doi.org/10.1021/bc300632w | *Bioconjugate Chem.* 2013, 24, 658−668

ethyl-3-(3-dimethylaminopropyl) carbodiimide (EDC), 90 mg (0.64 mmol) of hydroxybenzotriazole (HOBT), 80 μL of TEA, and 10 mg of 4-dimethylaminopyridine (DMAP) at continuous stirring under argon. After 4 h of reaction at 25 °C, a cholesteryl-amine linker (384 mg, 0.64 mmol) dissolved in 10 mL of DMSO was added, and the reaction mixture was stirred for 2 days at 25 °C. The product (CHA) was dialyzed in semipermeable tubes (MWCO 12−14 kDa) against water three times for 24 h at 25 °C and then concentrated *in vacuo*. CHA was dissolved in a small volume of methanol and purified by gel filtration on a Sephadex LH-20 column, using methanol as an eluent, with a yield of 85% after concentration *in vacuo*.

Synthesis of Drug Conjugates. CHA (100 mg, 0.25 mmol carboxyl groups) was dried by coevaporation with anhydrous toluene *in vacuo* and dissolved in 5 mL of anhydrous DMSO containing 42 μL (0.25 mmol) of *N,N*-diisopropylethylamine (DIPEA). Separately, 44 mg (0.075 mmol) of etoposide (ETO), 56 mg of salinomycin (SAL), or 28 mg of curcumin (CUR) was dried with 2 mg of DMAP by coevaporation with anhydrous toluene *in vacuo* and mixed with the CHA solution at the drug to CHA molar ratio of 30:1. Then, *N,N*-dicyclohexylcarbodiimide (DCC, 16 mg, 0.075 mmol) in 0.5 mL of anhydrous DMSO was added, and the reaction mixture was stirred for 3 days at 25 °C under argon. Water (10 μL) was added to stop the reaction, and the mixture was left overnight at 4 °C. The solution was filtered, dialyzed against water (MWCO 12−14 kDa), and concentrated *in vacuo*. CHA−drug conjugates were isolated by gel filtration on a Sephadex LH-20 column in methanol as an eluent. When dissolved in water, the pH of the CHA−drug conjugates was adjusted to 7, and finally, they were dialyzed against water overnight at 4 °C and lyophilized with a yield of 65−75%. The same procedure was used for the synthesis of nonmodified HA−drug conjugates.

Synthesis of Rhodamine-Labeled HA and CHA−Drug Conjugates. HA− or CHA−drug conjugate (100 mg) was dissolved in DMSO containing 2 mg of EDC, 2 mg of HOBT, 20 μL of TEA, and 2 mg of DMAP, and the reaction mixture was stirred for 4 h at 40 °C. Then 10 mg of 2,2′-(ethylenedioxy)-bis-ethylamine linker (L) was added, and the reaction was continued for 2 h at 25 °C. The product was dialyzed against water overnight and concentrated *in vacuo*, and the pH of the solution was adjusted to 8 by carbonate buffer. Rhodamine B isothiocyanate (3 mg) was dissolved in 50% aqueous dimethylformamide (DMF) and added to the above solution, and the reaction mixture was stirred overnight at 25 °C. Rhodamine-labeled Rh-HA or Rh-CHA−drug conjugates were dialyzed against water for 2 days at 4 °C and lyophilized.

Characterization of CHA−Drug Conjugates. Quantitative analysis of the cholesterol and drug content was performed by using ^{1}H NMR spectroscopy. ^{1}H NMR spectra were recorded in *d*-DMSO at 25 °C using a 500 MHz Varian NMR spectrometer. All chemical shift values are given in parts per million (ppm) and are referenced to a signal from tetramethylsilane. The ^{1}H NMR spectrum of CHA-ETO contained signals (see Supporting Information, Figure 1): 0.65 (s, 36H), 0.835−1.66 (m, 336H), 1.8 (m, 459H), 3.06−3.54 (m, 1925H), 4.05−4.08 (m, 22H), 4.23−5.22 (m, 963H), 6.01−6.03 (d, J = 10 Hz, 44H), 6.17 (s, 44H), 6.52 (s, 22H), 6.99 (s, 22H). The integrated signals for cholesterol methyl group (0.65 ppm), *N*-acetyl group of HA (1.8 ppm), and aromatic ring of etoposide (6.17 ppm) have been selected for the calculation of cholesterol and ETO content. The ^{1}H NMR spectrum of CHA-SAL contained signals (see Supporting Information, Figure 2): 0.65−1.64 (m, 454H), 1.84 (m, 459H), 3.00−3.94 (m, 1844H), 4.42−4.97 (m, 765H), 5.89 (d, J = 11 Hz, 23H), 6.15 (d, J = 10.5, 23H). The integrated signals for the *N*-acetyl group of HA (1.84 ppm) and tetrahydropyranyl ring of salinomycin (5.89 ppm, 6.15 ppm) have been selected for SAL content calculation. The ^{1}H NMR spectrum of CHA-CUR (see Supporting Information, Figure 3): 0.65−1.66 (m, 264H), 1.80(m, 459H), 3.00−3.83(m, 1997 H), 4.10−5.12(m, 963 H), 5.32 (6H), 6.05(s, 12H), 6.73(d, J = 16 Hz, 2H), 6.83(d, J = 8 Hz, 2H), 7.15(d, 8 Hz, 12 H), 7.318(s, 12 H), 7.557(d, J = 16 Hz, 12H). The integrated signals for the *N*-acetyl group of HA (1.8 ppm) and aromatic ring of curcumin (7.15 ppm) have been selected for CUR content calculation.

These CHA−drug conjugates formed compact nanogels after ultrasonication in aqueous solution. Usually, 30 min of treatment in bath sonicator was sufficient to obtain small uniform particles. The particle size, polydispersity, and zeta-potential of these nanogels were measured by dynamic light scattering (DLS) using Zetasizer Nano-ZS90 (Malvern Instruments, Southborough, MA) with a 15 mV solid state laser operated at a wavelength of 635 nm. The morphology and diameter of nanogel particles were also determined by transmission electron microscopy (TEM) after contrast staining with vanadate using a FEI Tecnai G2 Spirit instrument.

***In Vitro* Drug Release and Stability Study.** *In vitro* drug release was performed as follows. Solutions of CHA−drug nanogels (10 mg in 1 mL) were placed in small dialysis tubes (MWCO 3k) and immersed in 50 mL of PBS (pH 7.4) containing 0.1% sodium azide. During incubation at 25 °C under slow stirring, 100 μL samples were withdrawn from the PBS buffer at selected time points, and their UV absorbance was measured at 280 nm in triplicate using NanoDrop (ThermoScientific, Waltham, MA). Serial dilutions of drugs have been measured at 280 nm to obtain standard curves used to calculate the amount of drug released from the nanogel. Data were expressed in the form of cumulative drug release vs incubation time.

Degradation of curcumin can be detected by the significant reduction of its absorbance at λ_{max} 426 nm. In curcumin stability studies, CHA-CUR nanogel (2 mg/mL) and CUR solutions in PBS, pH 7.4, were incubated at 25 °C. At selected time points, UV spectra have been measured using SpectraMax M2Microplate Reader (Molecular Devices, USA).

***In Vitro* Cytotoxicity Assays.** The cytotoxicity of CHA− and HA−drug conjugates and free drugs was determined in cancer cell lines using a standard MTT assay. Briefly, 100 μL of cell suspension was seeded in flat-bottomed 96-well plates at a density of 5 000 cells/well. Cells were allowed to attach at 37 °C overnight, and then 100 μL of sample solutions at serial dilutions in full medium were added. Cells were incubated for 72 h at 37 °C, and the metabolic activity of samples was determined by adding 20 μL of MTT solution (5 mg/mL) in sterile PBS to each well. Plates were incubated for 4 h at 37 °C and centrifuged (500*g*, 5 min) to remove the medium. Then, 100 μL of extraction buffer (20% w/v SDS in 50% DMF, pH 4.7) was added to each well. Samples were incubated for 24 h at 37 °C. Optical absorbance at 560 nm was measured using a Model 680 microplate reader (BioRad, Hercules, CA). All cytotoxicity data were obtained from parallel sample measurements (n = 8) and plotted as survival percentage compared to control nontreated cells vs drug/nanogel concentrations. Data were converted into IC_{50} values (concentration of the 50% cell survival).

dx.doi.org/10.1021/bc300632w | *Bioconjugate Chem.* 2013, 24, 658−668

Scheme 1. Synthesis of cholesteryl hyaluronic acid−drug conjugates

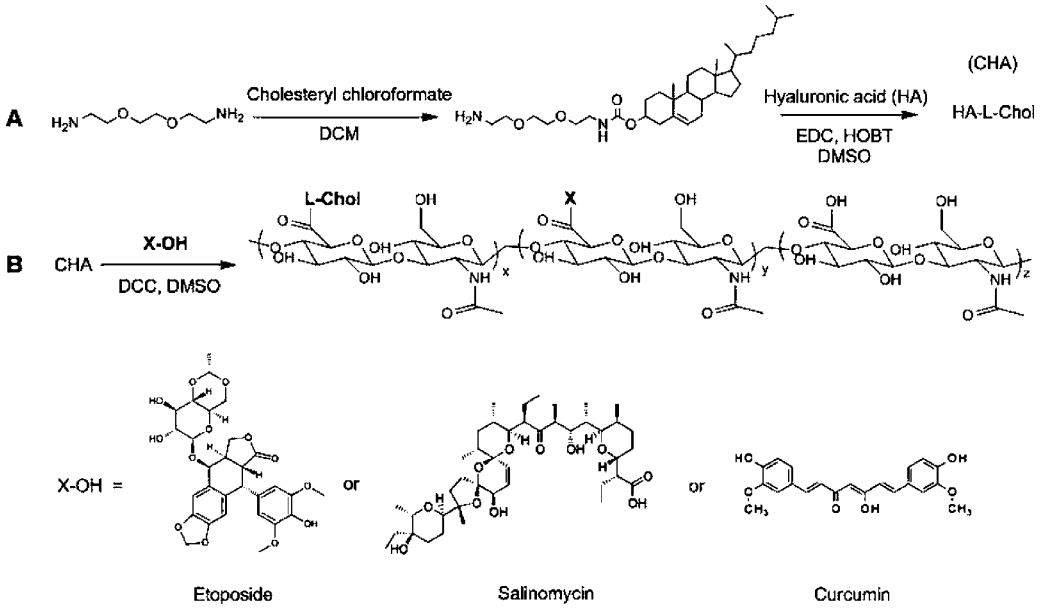

The lactate dehydrogenase (LDH) assay kit II (BioVision, San Diego, CA) was used to evaluate the cytotoxicity of nanogels in tumor spheroids according to the manufacturer's instructions. In brief, cancer cell spheroids were treated in 96-well plates with free drug, HA−drug conjugates, and CHA−drug nanogel. Two rows of control nontreated cells were set up. In the low control, no cell lysis buffer was used. In the high control, cells were treated with 10 μL of cell lysis buffer per well for 15 min. Cells were precipitated by centrifugation, and the culture medium was collected and treated with LDH Reaction Mix solution for 30 min at 25 °C. After the absorbance of controls and samples was measured at 450 nm, cytotoxicity as a percentage of dead cells was calculated using the following equation:

$$\text{cytotoxicity (\%)} = (\text{sample} - \text{low control}) / (\text{high control} - \text{low control}) \times 100$$

Flow Cytometry. CD44 expression levels in MDA-MB-231/F, MCF-7, and MIA PaCa-2 cells were determined using an allophycocyanin (APC)-conjugated mouse antihuman CD44 antibody (BD Pharmingen). Cells were washed once with PBS and then harvested with 0.05% trypsin/0.025% EDTA. Detached cells were washed and resuspended in wash buffer containing PBS, 1% FBS, and 1% penicillin/streptomycin (10^6 cells/100 μL). Fluorochrome-conjugated monoclonal antibody against human CD44 was added to the cell suspension at the concentration recommended by the manufacturer and incubated at 4 °C in the dark for 30 min. The antibody-labeled cells were washed in the wash buffer and fixed in PBS containing 1% paraformaldehyde, and then analyzed by flow cytometry on FACS Vantage (BD Biosciences).

Cellular Uptake. In cellular uptake experiments, cells were seeded in black-walled plates, and hodamine-labeled conjugates were added at different concentrations in triplicate. Plates were incubated at 37 °C for 2 h, washed 3 times with ice cold PBS, and treated with cell lysis buffer for 10 min. Fluorescence in the samples was measured using a BioTek FLx-800 fluorescence plate reader. A similar procedure was performed in time-dependence studies, where rhodamine-labeled conjugates (50 μg per well) were used in cell treatment, and cell samples were obtained at different time points in triplicate.

In order to investigate whether the uptake of CHA conjugates was CD44-dependent endocytosis, we carried out energy depletion and competitive inhibition studies. In the energy depletion study, cells were incubated at 4 and 37 °C. Rh-CHA uptake was measured as described above. In the competitive inhibition study, cells were pretreated with free HA (2 mg/mL, pH 7.4) for 1 h, washed, and treated with Rh-CHA (50 μg per well) in quadruplicate for 2 h at 37 °C. The uptake was compared with that of cells without pretreatment. The uptake of free carriers HA and CHA without drugs was similarly measured.

The uptake in living cells was visualized under each condition by confocal microscopy using Zeiss 510 Meta Confocal Laser Scanning Microscope.

Multicellular Cancer Spheroids (MCS). To prepare plates for the cultivation of MCS, we used the following protocol.[32] One gram of poly(2-hydroxyethyl methacrylate) (poly-HEMA) was dissolved in 50 mL of 95% ethanol overnight. The solution was clarified by centrifugation (2,000g, 10 min) and applied in 96-well U-bottomed culture plates (50 μL per well). The plates were dried overnight in a sterile hood under UV light, rinsed with PBS, and used for the cultivation of MCS. In all assays, the spheroids were formed 2 days after inoculation and maintained in complete MammoCult Medium (StemCell Technology, USA) including 0.0004% of heparin and 1 μM of hydrocortisone. These spheroids were cultured to the size 200−400 μm before living cell conditions studies. Penetration of Rh-CHA-ETO in spheroids was monitored by confocal laser scanning microscopy. For cytotoxicity studies, spheroids were incubated with CHA-ETO and then treated as described above.

Statistical Analysis. Statistical analysis was performed by application of the two-tailed unpaired Student's t test using SPSS 16.0 software. Differences between groups were considered significant at $P < 0.05$.

dx.doi.org/10.1021/bc300632w | *Bioconjugate Chem.* 2013, 24, 658−668

Scheme 2. Assembly of Compact CHA Nanogels in Aqueous Media and the Proposed Mechanism of Drug Delivery via Nanogel Binding with CD44 Receptors Expressed on the Membrane of Cancer Cells: Receptor-Mediated Endocytosis and the Fusion of CHA−Drug Conjugates in the Lipid Bilayer

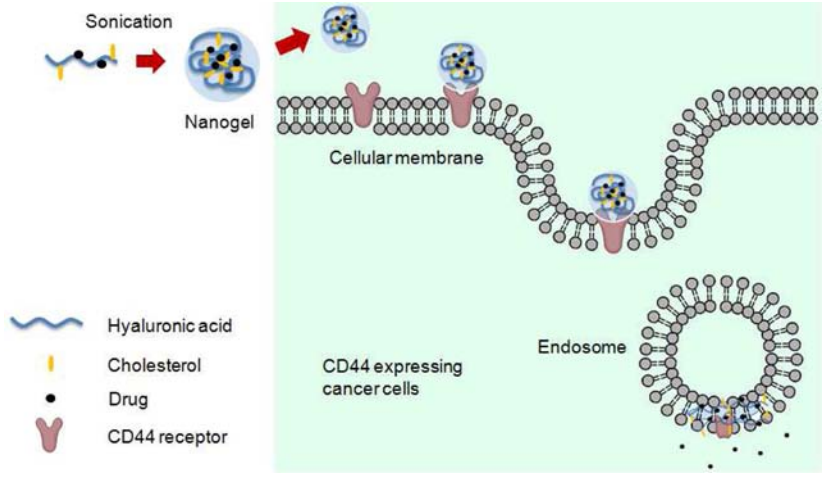

Table 1. Characterization of Obtained Formulations[a]

nanogel	size (nm)	PDI	drug content by weight (%)	cholesterol content by weight (%)	zeta potential (mV)
CHA-ETO	32.17 ± 5.66	0.28 ± 0.03	17.36 ± 1.21	3.42 ± 0.04	−31.6 ± 2.61
CHA-SAL	36.48 ± 6.23	0.29 ± 0.05	21.62 ± 1.53	3.38 ± 0.04	−41.4 ± 4.52
CHA-CUR	29.15 ± 5.37	0.45 ± 0.06	6.98 ± 0.56	3.85 ± 0.05	−38.4 ± 3.89

[a]PDI: polydispersity index. Values are the mean ± standard deviation (SD) (n = 3).

RESULTS AND DISCUSSION

Synthesis and Characterization of HA-Based Drug Conjugates. We synthesized cholesteryl-hyaluronic acid−drug conjugates as shown in Scheme 1A. It was earlier determined that the CD44-binding efficacy of HA depends on its M_w and that the stable binding occurs with HA having a M_w of at least 30 kDa.[22] Here, we chose the HA with M_w of 60 kDa in order to obtain smaller nanogels with sufficient drug-loading capability and good CD44-binding efficacy. Following the modification with cholesterol, amphiphilic CHA conjugates could form compact nanogels (<100 nm in diameter) after ultrasonication in aqueous media. Previously, we observed that the degree of modification of hydrophilic cationic nanogels with cholesterol chloroformate must be between 3 and 10% in order to ensure good solubility and effective cellular uptake of cholesteryl-nanogels.[23] Here, we used a cholesteryl-amine linker (L) synthesized from 2,2′-(ethylenedioxy)-bis-ethylamine in order to obtain a stable CHA nanogel (Scheme 2A). This linker was used for the modification of carbodiimide-activated carboxyl groups in a 6-fold molar excess over HA molecule. ^{1}H NMR analysis confirmed the high reaction efficacy: the cholesterol content in CHA was equal to 3.5 ± 0.3% or 5.9 cholesterol molecules in average per HA polymer. It was in good correlation with the input amount of the cholesteryl-amine linker used in the synthesis (Table 1).

In the second step, the CHA nanogel was covalently conjugated to etoposide, salinomycin, or curcumin through the formation of degradable ester bonds. As shown in Scheme 1B, carboxyl groups of CHA were activated by dicyclohexylcarbodiimide (DCC) and coupled with the above-mentioned drugs in anhydrous conditions.[24] The final drug content in conjugates directly depended on the input amount of drug used in the coupling (Table 1). The CHA−drug nanogels could be obtained with higher drug loading compared to many liposomal drug formulations (7−11%).[7,14] We demonstrated that drug solubility could be elevated by at least 100 times when CHA−drug nanogels are used.

Nanogel Formation. The synthesized CHA−drug conjugates readily formed compact nanogels after ultrasonication in aqueous media. Usually, 30−60 min treatment in a bath sonicator (70W, 42 kHz ± 6%) was sufficient to obtain uniform nanogel particles mostly free of aggregates. Particle size, polydispersity, and morphology of nanogels were investigated by dynamic light scattering and transmission electron microscopy (Table 1 and Figure 1). All three nanogel−drug conjugates formed small particles with a spherical morphology, narrow size distribution, and hydrodynamic diameters between 29 and 40 nm. HA−drug conjugates formed much larger particles (see Supporting Information, Table 1). The zeta-potential of all nanogels was negative (Table 1) due to the high amount of carboxyl groups in HA. Compared to HA-grafted liposomes having a diameter of 120−180 nm[14] or HACE nanoparticles with particle sizes more than 100 nm,[16,17] CHA−

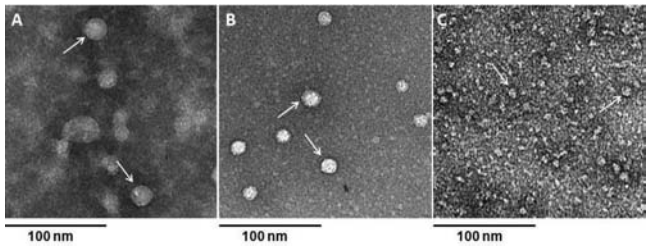

Figure 1. Transmission electron microscopic images of CHA nanogels: (A) CHA-ETO, (B) CHA-SAL, and (C) CHA-CUR. Samples were stained with vanadate. Selected nanogel particles are shown by arrows.

dx.doi.org/10.1021/bc300632w | Bioconjugate Chem. 2013, 24, 658−668

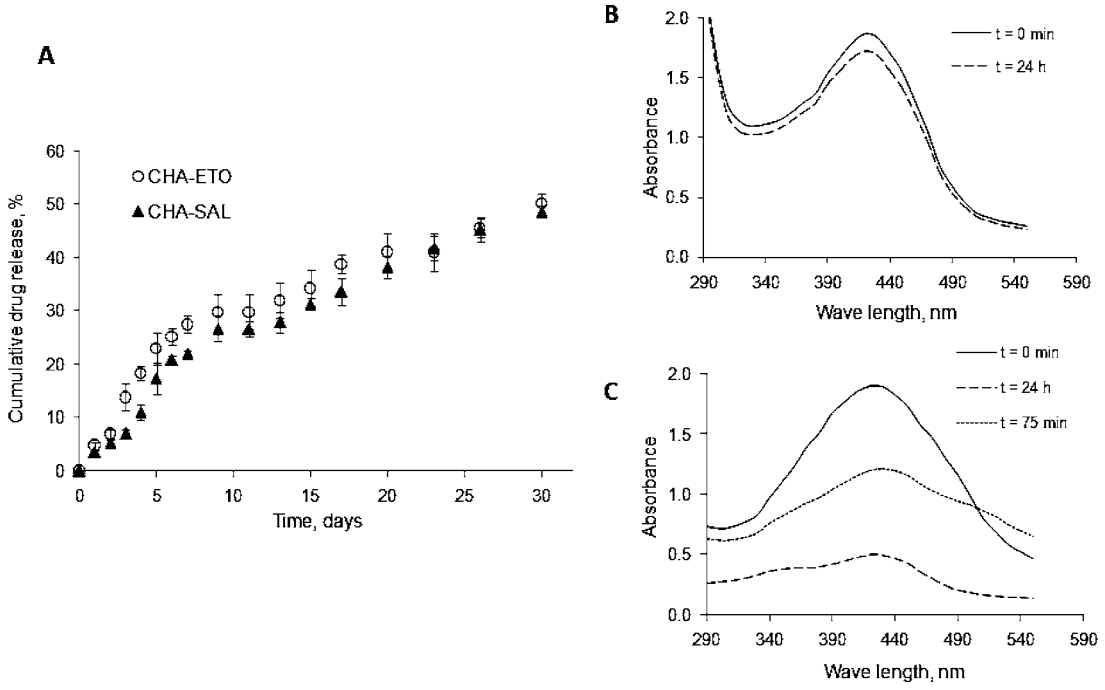

Figure 2. *In vitro* drug release and stability in nanogel−drug conjugates. (A) Drug release of CHA-ETO and CHA-SAL at pH 7.4, 37 °C. Data are expressed as the means ± SD (n = 3). (B,C) Comparison of the drug stability for CHA-CUR (B) and free CUR (C) at pH 7.4, 25 °C, and [CUR] = 110 μM. The UV absorbance decrease at λ_{max} of CUR = 426 nm shows the degradation of CUR molecules.

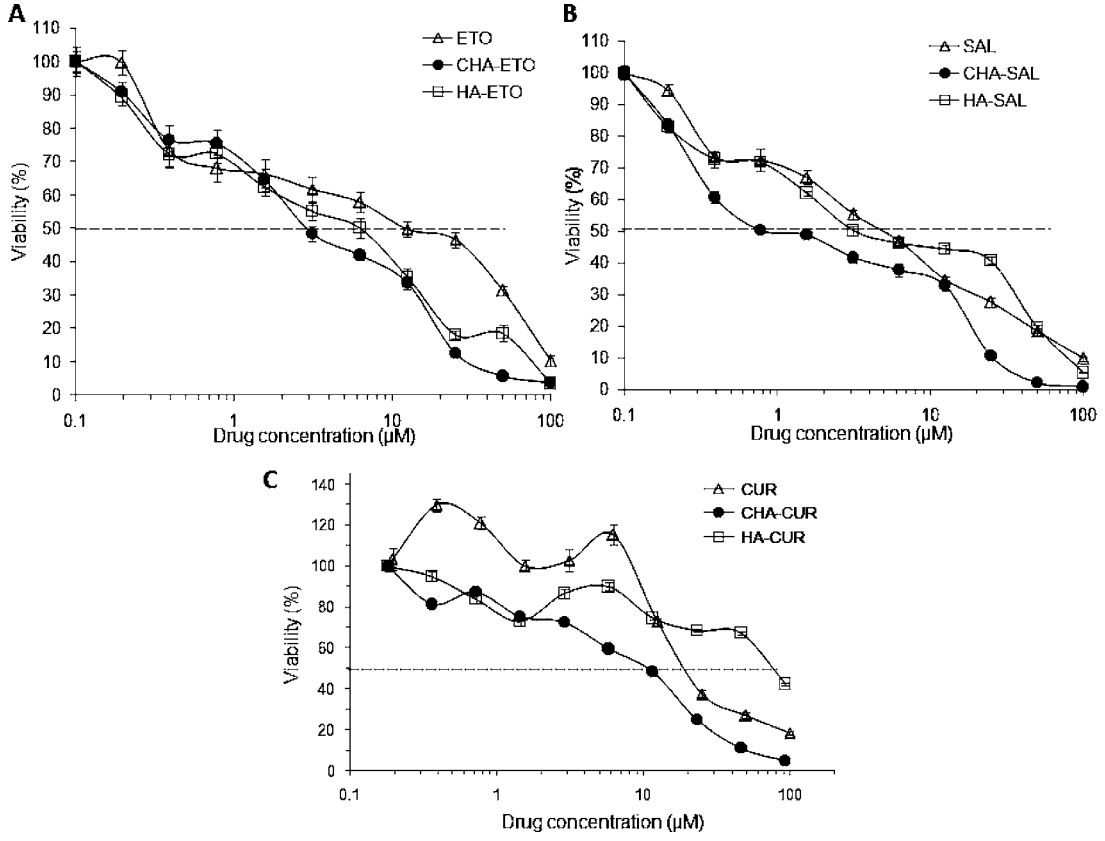

Figure 3. Comparative cytotoxicity of CHA nanogel−drug conjugates vs HA−drug conjugates and free drugs in MDA-MB-231/F (A,B) and MIA PaCa-2 (C) cells (MTT assay, 72 h, 37 °C). Data are shown as the means ± SEM (n = 8).

drug nanogels have significantly lower particle sizes. For the efficient accumulation in tumor tissue via enhanced permeability and retention (EPR) effect, nanocarriers should be smaller than 200 nm since nanocarriers larger than 200 nm are predominantly cleared by the reticuloendothelial system (RES).[25] The smaller size is a prerequisite for the efficient

dx.doi.org/10.1021/bc300632w | *Bioconjugate Chem.* 2013, 24, 658−668

penetration of nanocarriers into the tumor mass, as well as their transport through the gastrointestinal barrier where the absorption of nanoparticles was 15−250 times than that of the microparticles.[35]

***In Vitro* Drug Release and Stability.** The *in vitro* drug release from CHA−drug nanogels was monitored at 37 °C and pH 7.4 in order to assess nanogel stability in physiological conditions. Both CHA-ETO and CHA-SAL nanogels showed practically identical slow release profiles with a mean release rate of 1.6−1.7% per day (Figure 2A). Since the major problems of therapeutic curcumin are its low solubility and rapid degradation in physiological conditions,[26] we monitored the drug stability in CHA-CUR nanogel by the drop in absorbance at 430 nm (Figure 2B). The UV spectrum of CHA-CUR solution showed less than 10% drug degradation after 24 h of incubation at pH 7.4. In the same conditions, most of the free curcumin was degraded during that time (Figure 2C). It was earlier demonstrated that esterification of curcumin significantly increased its stability to oxidation in neutral conditions.[36]

Cytotoxicity. We compared the cytotoxicity of CHA−drug nanogels, HA−drug conjugates, and free drugs in drug-resistant human breast carcinoma MDA-MB-231/F (selected by resistance to floxuridine) and pancreatic adenocarcinoma MIA PaCa-2 (medium gemcitabine-resistant) cells using a thiazolyl blue (MTT)-based cytotoxicity assay (Figure 3). CHA−drug nanogels demonstrated lower IC_{50} values compared to both free drugs and HA−drug conjugates as shown in Table 2. We calculated the enhancement factor (EF), which is defined as IC_{50} (drug)/IC_{50} (drug formulation). The EF values of CHA-ETO, CHA-SAL, and CHA-CUR were equal to 4.2, 5.4, and 2.1, respectively. Furthermore, the cytotoxicity of CHA-ETO, CHA-SAL, and CHA-CUR nanogels was also 2.1, 3.4, and 7.8 times higher compared to those of the HA-ETO, HA-SAL, and HA-CUR conjugates, respectively. Meanwhile, the CHA empty nanogel demonstrated a negligible cytotoxicity (IC_{50} > 5 mg/mL). Thus, the application of CHA nanogels not only improved particle size but also significantly enhanced the anticancer efficacy of conjugated drugs.

Table 2. Cytotoxicity of Drugs and Drug Conjugates in Cancer Cells

drug formulations	IC_{50} value (μM)[a]	enhancement factor
etoposide	12.3	
HA-ETO	6.3	1.9
CHA-ETO	3	4.2
salinomycin	5.1	
HA-SAL	3.2	1.6
CHA-SAL	0.9	5.4
curcumin	19	
HA-CUR	70	0.3
CHA-CUR	9	2.1

[a]Cytotoxicity was measured after 72 h of treatment. The enhancement factor shows the drug conjugate efficacy compared to that of the free drug. CHA cytotoxicity (IC_{50}) was >5 mg/mL. The data are the average of eight parallel measurements. Etoposide and salinomycin conjugates were tested in MDA-MB-231/F cells; curcumin conjugates were tested in MIA PaCa-2 cells.

Intracellular Uptake. Cellular accumulation of HA is driven by energy-dependent CD44 receptor-mediated endocytosis, although the mechanism of it is not yet fully understood.[27] Here, we evaluated the effects of cholesterol substitution on the cellular uptake of rhodamine-labeled CHA nanogel in cancer cells expressing different levels of CD44. Analysis of CD44 expression by flow cytometry demonstrated that human breast carcinoma MCF-7 cells expressed the lowest CD44 level, while MDA-MB-231/F and MIA PaCa-2 demonstrated 15 times and 29 times higher CD44 levels, respectively (Figure 4B). Confocal microscopy showed an active nanogel accumulation in MDA-MB-231/F cells at 37 °C that was significantly suppressed at 4 °C (Figure 4A,a-b). A 40% decline in accumulation was confirmed by direct measurements of fluorescence normalized for the same amount of cells (Figure 4C,a). Thus, the cellular uptake of CHA nanogels was, at least partly, an energy-dependent process of receptor-mediated endocytosis. Pretreatment of cells with free HA also resulted in the partial inhibition of CHA nanogel accumulation, which supports the direct involvement of the receptor-mediated mechanism of uptake (Figure 4A,c and C,b). Direct comparison of rhodamine-labeled HA and CHA showed that the uptake of the CHA nanogel was at least 20% more efficient (Figure 4A,d and C,c). Evidently, the interaction of cholesterol moieties with the cellular membrane plays a prominent role in cellular internalization of CHA nanogels. A reduced level of CHA nanogel accumulation was observed in MCF-7 cells that expressed significantly lower CD44 levels compared to those of MDA-MB-231/F (Figure 4A,e and C,d).

Vectorized nanocarriers are internalized mostly by receptor-mediated endocytosis. Endosome-sequestered nanocarriers are then transferred into lysosomes, where they are digested and have their cargos degraded, and the remains are finally recycled out of cells.[27] Acid labile linkers (hydrazone and ester groups) are usually introduced in prodrugs to facilitate intracellular drug release since late endosomes and lysosomes have pH values in the range of 5.0−5.5.[28] Hydrophilic prodrugs like HA−drug conjugates may remain in the endosome and degrade or recycle later. In contrast, the CHA−drug nanogels provide strong advantage in more effective drug delivery since they can easily unfold on the membrane surface after receptor-mediated endocytosis by anchoring in the lipid bilayer via multiple cholesterol moieties. Thus, the superior cytotoxic efficacy of CHA−drug conjugates compared to that of HA−drug conjugates in cancer cells can be explained by this ability to fuse with the cellular membrane and form semipermeable patches allowing fast drug release in the cytoplasm as shown in Scheme 2. A similar mechanism of drug release including the fusion with the cellular membrane was previously identified for cationic nanogels that delivered hydrophilic drugs otherwise incapable of penetrating the lipid bilayer.[29] The main location of the CD44 receptor is on lipid rafts that are rich in cholesterol as a previous report suggested.[30] Potentially, both interactions with lipid rafts and CD44 receptors could work in concert for CHA nanogels to enhance the intracellular drug delivery. Our results show that the accumulation of CHA nanogels is a process where nearly equal parts are determined by CD44-mediated endocytosis and the cholesterol-related interaction with the membrane of cancer cells. The CHA accumulation levels correlated well with the CD44 expression in different cell lines. Accumulation of HA-engrafted liposomes and HACE-based nanoparticles was also CD44-dependent.[14,16] Thus, the direct comparison of HA polymer and CHA nanogels demonstrated that cholesterol modification is the major factor in the observed higher cellular accumulation of CHA nanogels and stronger cytotoxicity of CHA nanogel−drug conjugates.

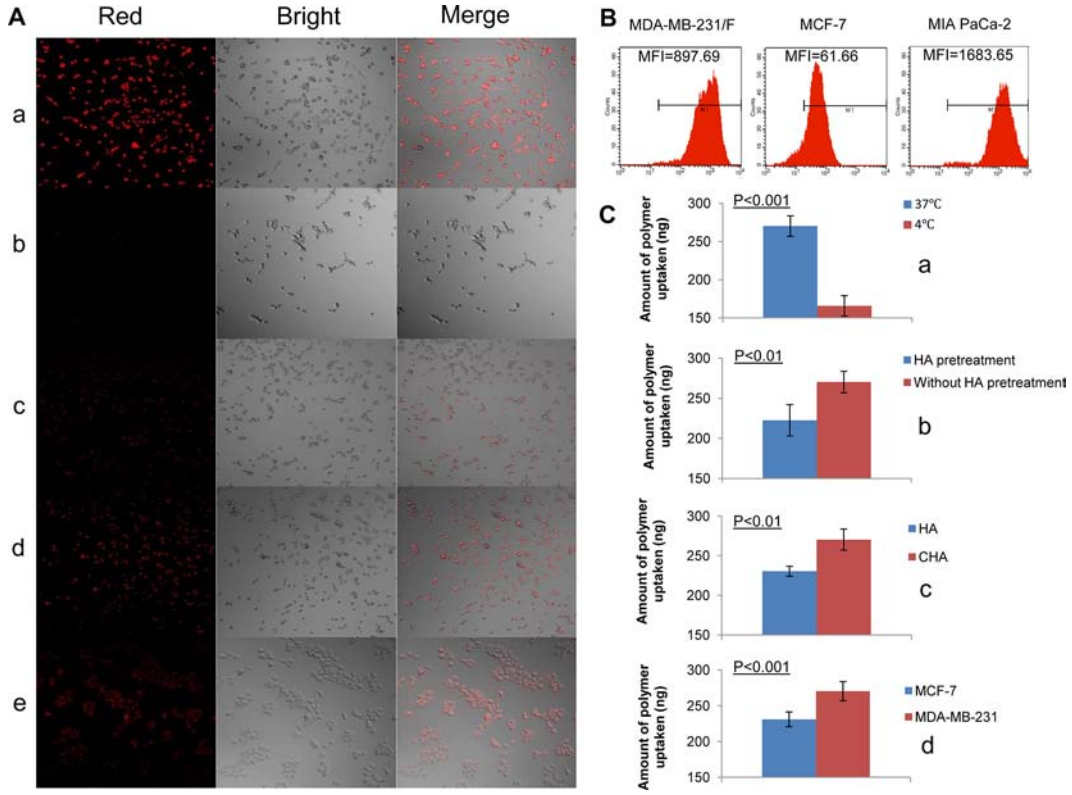

Figure 4. Cellular uptake of rhodamine-labeled HA and CHA nanogels. (A) Confocal microscopy of (a) MDA-MB-231/F cells incubated with Rh-CHA for 2 h at 37 °C. (b) MDA-MB-231/F cells incubated with Rh-CHA for 2 h at 4 °C. (c) MDA-MB-231/F cells pretreated with free HA and then incubated with Rh-CHA for 2 h at 37 °C. (d) MDA-MB-231/F cells incubated with Rh-HA for 2 h at 37 °C. (e) MCF-7 cells incubated with Rh-CHA for 2 h at 37 °C. (B) CD44 expression in MDA-MB-231/F, MCF-7, and MIA PaCa-2 cells determined by flow cytometry. MFI: mean fluorescence index. (C) Quantitative comparison of the cellular uptake of fluorescent Rh-CHA measured per 50,000 cells: (a) at 4 °C vs 37 °C, (b) with or without pretreatment by HA, (c) HA vs CHA, and (d) MCF-7 vs MDA-MB-231/F. Data are expressed as the means ± SEM.

Penetration and Cytotoxicity of CHA Nanogels in Cancer Spheroids. A 3D-culture of multicellular cancer spheroids (MCS) was proposed as a better model for drug efficacy testing than cellular monolayers since the MCS cultures share many properties of solid tumors, such as the development of an extracellular matrix (ECM), nutritional concentration gradients, and the outer layer-to-core cell proliferation.[31] MCS may consist of proliferating, quiescent, and necrotic core regions and form oxygen and glucose gradients similar to those of solid tumors. MCS models also demonstrated higher drug resistance and tumor-like penetration of therapeutic molecules as compared to cellular monolayers. Many hydrophobic drugs are bound only to the outer layers of MCS, which results in poor drug transport into inner parts of the MCS. Obviously, encapsulation of hydrophobic drugs in hydrophilic nanocarriers can make the process more efficient.

Here, we examined the penetration and cytotoxic activity of CHA−drug nanogels in 3D-cultures of MCF-7 and MIA PaCa-2 MCS. The spheroids were grown for several days to the size of 300−400 μm in low adhesion plates and at low-serum conditions.[32] After supplementing the MCS with full medium, they were incubated with rhodamine-labeled CHA-ETO and CHA-SAL. As shown by confocal microscopy, both nanogel−drug conjugates could penetrate MCF-7 MCS by 50−60 μm after 12 h of incubation (white arrow), a penetration rate equal to 4−5 μm per hour (Figure 5A,B). An average area of MCF-7 cells is 400 μm^2 or 20 × 20 μm^2. Thus, the nanogel can penetrate through up to 6 cell layers per day. For most MCS, it would take approximately three days for CHA nanogel−drug conjugates to penetrate to the core. Along with penetration, CHA nanogels could bind CD44 receptors and rapidly internalize into cancer cells and kill them (Figure 5C). Their very small size was a positive factor enhancing the CHA nanogel−drug efficacy; previous experiments with larger nanocarriers demonstrated very slow penetration.[33]

To compare the cytotoxicity of CHA-ETO and HA-ETO, we measured the extracellular release of lactate dehydrogenase (LDH) caused by the rupture of the cellular membrane in apoptotic and dead cells following 48 h of treatment with MIA PaCa-2 MCS. Cytotoxicity was expressed as a percentage of dead cells in the total MCS cell amount. The cytotoxicity of free ETO and CHA-ETO was mostly equal and significantly higher than the cytotoxicity of HA-ETO at all drug doses. CHA-ETO demonstrated 2-fold and 4-fold better cytotoxic effect against MCS compared to that of ETO and HA-ETO, respectively, at a higher dose (Figure 6A).

The spheroid penetration ability and the cellular uptake rate could be considered as two major impact factors on the observed cytotoxicity. Hydrophobic ETO has a less efficient diffusion and can also be eliminated from cancer cells by P-glycoprotein, thus reducing the overall cytotoxic effect.[37] In our experiment, the increasing dose does not very efficiently improve the penetration and cytotoxicity of ETO alone compared to that of CHA-ETO. First, the CHA-ETO nanogel can overcome drug resistance by shielding the drug inside the carrier. Second, CHA-ETO cytotoxicity was different in cell lines that express different CD44 levels (Figure 6B). MIA PaCa-2 cells have a high level of CD44 expression level, while

dx.doi.org/10.1021/bc300632w | Bioconjugate Chem. 2013, 24, 658−668

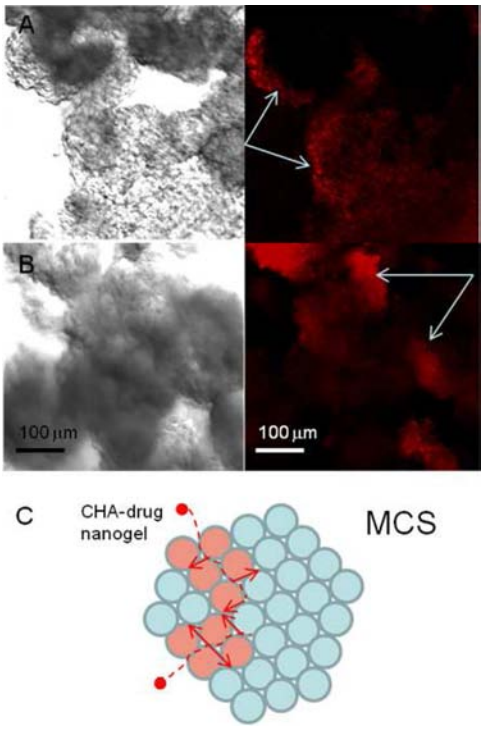

Figure 5. Penetration of rhodamine-labeled CHA-ETO (A) and CHA-SAL (B) in MCF-7 multicellular cancer spheroids (MCS) detected by confocal microscopy (12 h, 37 °C). White arrows show nanogel penetration (left, contrast image; right, fluorescent image; side length, 500 μm). (C) Schematic view of nanogel penetration into MCS and accumulation in adjacent cells.

MCF-7 cells express low CD44 levels, and both cell lines easily form MCS during 3D-culturing. CHA-ETO displayed 40% lower cytotoxicity in MCF-7 cells than in MIA PaCa-2 cells, and the cytotoxicity was dose-dependent in both MCS types. The CHA-ETO cytotoxicity at a constant dose (25 μg/mL) was exponentially elevated at longer incubation time in both MCS types, obviously, due to the overlapping of inner penetration in MCS and cellular accumulation of drug (Figure 6C). CHA-ETO nanogels were more effective against MIA PaCa-2 MCS as compared to MCF-7 MCS, which is in good correlation with CD44 expression levels in these cells, but nevertheless, the overall effect on both cell types was high.

CONCLUSIONS

We developed cholesteryl-hyaluronic acid (CHA) nanogel–drug conjugates for efficient treatment of cancer cells and, especially, drug-resistant and CD44-expressing cancer cells. In the design of CHA nanogel–drug conjugates, we focused on enhancement of various aspects of drug delivery, including drug solubility, loading capacity, nanogel size, drug release from nanogel in cytoplasm, and active tumor targeting. The stronger cytotoxicity of CHA–drug nanogels in cancer cells and spheroids compared to that of simple HA–drug conjugates was due to better cellular uptake determined by the higher affinity of CHA nanogels to the cellular membrane and only partly by the binding with CD44 receptors overexpressed in drug-resistant cancer cells. We also demonstrated the fast penetration and high therapeutic activity of CHA nanogel–drug conjugates in 3D-cultures of multicellular cancer spheroids. In conclusion, CHA nanogel–drug conjugates, as simple and effective macromolecular drugs, are suggested as promising candidates for the treatment of CD44-expressing tumors and, potentially, for the eradication of CSCs in the process of overcoming resistance to chemotherapy and tumor relapse.[34]

ASSOCIATED CONTENT

Supporting Information

Characterization data for HA–drug conjugates and ^{1}H NMR spectra of CHA-ETO, CHA-SAL, and CHA-CUR. This material is available free of charge via the Internet at http://pubs.acs.org.

AUTHOR INFORMATION

Corresponding Author

*986025, Nebraska Medical Center, Omaha, NE 68198-6025. Phone: (402) 559-9362. Fax: (402) 559-9543. E-mail: vinograd@unmc.edu.

Notes

The authors declare no competing financial interest.

ACKNOWLEDGMENTS

This work was supported by NIH grant R01 CA136921 (to S.V.V.) and Chinese Scholarship Council (to X.W.). We are also grateful to State Key Laboratory of Biotherapy and Cancer Center, West China Medical School, Sichuan University, China, for its support to X.W. Expert assistance of Tom Bargar (UNMC Electron Microscopy Core Facility), Victoria B. Smith

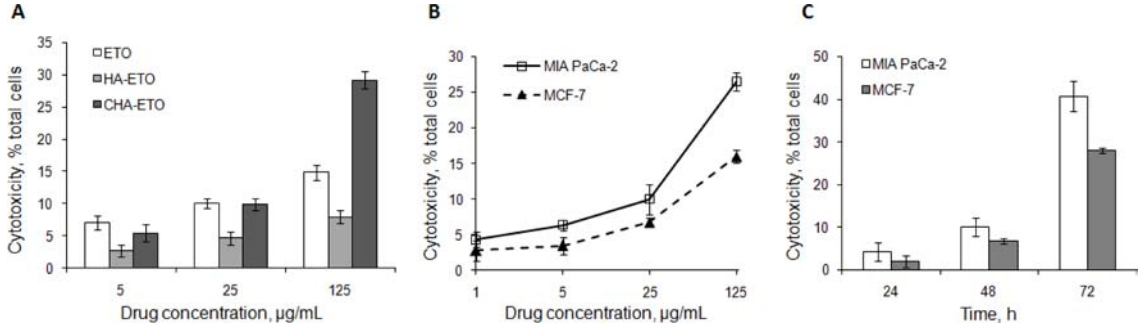

Figure 6. Comparative cytotoxicity of CHA-ETO, HA-ETO, and ETO in MCS. (A) MIA PaCa-2 MCS (treatment 48 h, 37 °C); $P < 0.05$, CHA-ETO vs ETO, and $P < 0.05$, CHA-ETO vs HA-ETO. (B) Dose-dependent cytotoxicity of CHA-ETO in MIA PaCa-2 and MCF-7 MCS (48 h, 37 °C). (C) Time-dependent cytotoxicity of CHA-ETO in MIA PaCa-2 and MCF-7 MCS (drug concentration 25 μg/mL); $P < 0.05$, MIA PaCa-2 vs MCF-7. Cytotoxicity was determined using LDH assay. Data are shown as the means ± SEM ($n = 5$).

(UNMC Cell Analysis Core Facility), Janice A. Taylor (UNMC Confocal Laser Scanning Microscopy Core Facility), and Ed Ezell (UNMC NMR Core Facility) is greatly appreciated.

■ ABBREVIATIONS

HA, hyaluronic acid; CHA, cholesteryl-HA; EBE, 2,2′-(ethylenedioxy)-bis-ethylamine; DCM, dichloromethane; TEA, triethylamine; CCF, cholesteryl chloroformate; EDC, 1-ethyl-3-(3-dimethylaminopropyl) carbodiimide; HOBT, hydroxybenzotriazole; DMAP, 4-dimethylaminopyridine; DCC, *N*,*N*′-dicyclohexylcarbodiimide; DMF, *N*,*N*-dimethylformamide; DMSO, dimethyl sulfoxide; DIPEA, *N*,*N*-diisopropylethylamine; RhITC, rhodamine B isothiocyanate; ETO, etoposide; SAL, salinomycin; CUR, curcumin; MTT, 3-[4,5-dimethylthiazol-2-yl]-2,5-diphenyltetrazolium bromide; FdU, 5-fluoro-2′-deoxyuridine

■ REFERENCES

(1) Baguley, B. C. (2010) Multiple drug resistance mechanisms in cancer. *Mol. Biotechnol. 46*, 308−316.

(2) Jordan, C. T., Guzman, M. L., and Noble, M. (2006) Cancer stem cells. *N. Engl. J. Med. 355*, 1253−1261.

(3) Vanneman, M., and Dranoff, G. (2012) Combining immunotherapy and targeted therapies in cancer treatment. *Nat. Rev. Cancer 12*, 237−51.

(4) Crosasso, P., Brusa, P., Dosio, F., Arpicco, S., Pacchioni, D., Schuber, F., and Cattel, L. (1997) Antitumoral activity of liposomes and immunoliposomes containing 5-fluorouridine prodrugs. *J. Pharm. Sci. 86*, 832−9.

(5) Kim, S., Shi, Y., Kim, J. Y., Park, K., and Cheng, J. X. (2010) Overcoming the barriers in micellar drug delivery: loading efficiency, in vivo stability, and micelle-cell interaction. *Expert Opin. Drug Delivery 7*, 49−62.

(6) Lu, Z. R., Shiah, J. G., Sakuma, S., Kopeckova, P., and Kopecek, J. (2002) Design of novel bioconjugates for targeted drug delivery. *J. Controlled Release 78*, 165−173.

(7) Senanayake, T. H., Warren, G., and Vinogradov, S. V. (2011) Novel anticancer polymeric conjugates of activated nucleoside analogues. *Bioconjugate Chem. 22*, 1983−1993.

(8) Stern, R., Asari, A. A., and Sugahara, K. N. (2006) Hyaluronan fragments: an information-rich system. *Eur. J. Cell Biol. 85*, 699−715.

(9) Prestwich, G. D. (2011) Hyaluronic acid-based clinical biomaterials derived for cell and molecule delivery in regenerative medicine. *J. Controlled Release 155*, 193−199.

(10) Luo, Y., Ziebell, M. R., and Prestwich, G. D. (2000) A hyaluronic acid-taxol antitumor bioconjugate targeted to cancer cells. *Biomacromolecules 1*, 208−218.

(11) Luo, Y., Bernshaw, N. J., Lu, Z. R., Kopecek, J., and Prestwich, G. D. (2002) Targeted delivery of doxorubicin by HPMA copolymer-hyaluronan bioconjugates. *Pharm. Res. 19*, 396−402.

(12) Marhaba, R., Klingbeil, P., Nuebel, T., Nazarenko, I., Buechler, M. W., and Zoeller, M. (2008) CD44 and EpCAM: cancer-initiating cell markers. *Curr. Mol. Med. 8*, 784−804.

(13) (15) Oh, E. J., Park, K., Kim, K. S., Kim, J., Yang, J. A., Kong, J. H., Lee, M. Y., Hoffman, A. S., and Hahn, S. K. (2010) Target specific and long-acting delivery of protein, peptide, and nucleotide therapeutics using hyaluronic acid derivatives. *J. Controlled Release 141*, 2−12.

(14) Qhattal, H. S., and Liu, X. (2011) Characterization of CD44-mediated cancer cell uptake and intracellular distribution of hyaluronan-grafted liposomes. *Mol. Pharmaceutics 8*, 1233−1246.

(15) Cho, H. J., Yoon, H. Y., Koo, H., Ko, S. H., Shim, J. S., Lee, J. H., Kim, K., Kwon, I. C., and Kim, D. D. (2011) Self-assembled nanoparticles based on hyaluronic acid-ceramide (HA-CE) and Pluronic(R) for tumor-targeted delivery of docetaxel. *Biomaterials 32*, 7181−7190.

(16) Cho, H. J., Yoon, I. S., Yoon, H. Y., Koo, H., Jin, Y. J., Ko, S. H., Shim, J. S., Kim, K., Kwon, I. C., and Kim, D. D. (2012) Polyethylene glycol-conjugated hyaluronic acid-ceramide self-assembled nanoparticles for targeted delivery of doxorubicin. *Biomaterials 33*, 1190−1200.

(17) Cho, H. J., Yoon, H. Y., Koo, H., Ko, S. H., Shim, J. S., Cho, J. H., Park, J. H., Kim, K., Kwon, I. C., and Kim, D. D. (2012) Hyaluronic acid-ceramide-based optical/MR dual imaging nanoprobe for cancer diagnosis. *J. Controlled Release 162*, 111−118.

(18) Boutorine, A., and Kostina, E. (1993) Reversible covalent attachment of cholesterol to oligodeoxyribonucleotides for studies of the mechanisms of their penetration into eucaryotic cells. *Biochimie 75*, 35−41.

(19) Nochi, T., Yuki, Y., Takahashi, H., Sawada, S., Mejima, M., Kohda, T., Harada, N., Kong, I. G., Sato, A., Kataoka, N., Tokuhara, D., Kurokawa, S., Takahashi, Y., Tsukada, H., Kozaki, S., Akiyoshi, K., and Kiyono, H. (2010) Nanogel antigenic protein-delivery system for adjuvant-free intranasal vaccines. *Nat. Mater. 9*, 572−578.

(20) Gupta, P. B., Onder, T. T., Jiang, G., Tao, K., Kuperwasser, C., Weinberg, R. A., and Lander, E. S. (2009) Identification of selective inhibitors of cancer stem cells by high-throughput screening. *Cell 138*, 645−659.

(21) Lim, K. J., Bisht, S., Bar, E. E., Maitra, A., and Eberhart, C. G. (2011) A polymeric nanoparticle formulation of curcumin inhibits growth, clonogenicity and stem-like fraction in malignant brain tumors. *Cancer Biol. Ther. 11*, 464−473.

(22) Wolny, P. M., Banerji, S., Gounou, C., Brisson, A. R., Day, A. J., Jackson, D. G., and Richter, R. P. (2010) Analysis of CD44-hyaluronan interactions in an artificial membrane system. *J. Biol. Chem. 285*, 30170−30180.

(23) Vinogradov, S. V., Kohli, E., Zeman, A., and Kabanov, A. V. (2006) Chemical engineering of nanogel drug carriers: increased bioavailability and decreased cytotoxicity. *Polym. Prepr. 47* (2), 27−28.

(24) Keck, G. E., Boden, E. P., and Wiley, M. R. (1989) Total synthesis of (+)-colletodiol: new methodology for the synthesis of macrolactone. *J. Org. Chem. 54*, 896−906.

(25) Yuan, F., Dellian, M., Fukumura, D., Leunig, M., Berk, D. A., Torchilin, V. P., and Jain, R. K. (1995) Vascular permeability in a human tumor xenograft: molecular size dependence and cutoff size. *Cancer Res. 55*, 3752−3756.

(26) Manju, S., and Sreenivasan, K. (2011) Conjugation of curcumin onto hyaluronic acid enhances its aqueous solubility and stability. *J. Colloid Interface Sci. 359*, 318−325.

(27) Tammi, R., Rilla, K., Pienimaki, J. P., MacCallum, D. K., Hogg, M., Luukkonen, M., Hascall, V. C., and Tammi, M. (2001) Hyaluronan enters keratinocytes by a novel endocytic route for catabolism. *J. Biol. Chem. 276*, 35111−35122.

(28) Yang, J., Chen, H., Vlahov, I. R., Cheng, J. X., and Low, P. S. (2007) Characterization of the pH of folate receptor-containing endosomes and the rate of hydrolysis of internalized acid-labile folate-drug conjugates. *J. Pharmacol. Exp. Ther. 321*, 462−468.

(29) Vinogradov, S. V., Kohli, E., and Zeman, A. D. (2005) Cross-linked polymeric nanogel formulations of 5′-triphosphates of nucleoside analogues: role of the cellular membrane in drug release. *Mol. Pharmaceutics 2*, 449−461.

(30) Oliferenko, S., Paiha, K., Harder, T., Gerke, V., Schwarzler, C., Schwarz, H., Beug, H., Gunthert, U., and Huber, L. A. (1999) Analysis of CD44-containing lipid rafts: Recruitment of annexin II and stabilization by the actin cytoskeleton. *J. Cell Biol. 146*, 843−854.

(31) Sutherland, R. M. (1988) Cell and environment interactions in tumor microregions: the multicell spheroid model. *Science 240*, 177−184.

(32) Huang, K., Ma, H., Liu, J., Huo, S., Kumar, A., Wei, T., Zhang, X., Jin, S., Gan, Y., Wang, P. C., He, S., and Liang, X. J. (2012) Size-dependent localization and penetration of ultrasmall gold nanoparticles in cancer cells, multicellular spheroids, and tumors in vivo. *ACS Nano 6*, 4483−4493.

(33) Kim, T. H., Mount, C. W., Gombotz, W. R., and Pun, S. H. (2010) The delivery of doxorubicin to 3-D multicellular spheroids and

tumors in a murine xenograft model using tumor-penetrating triblock polymeric micelles. *Biomaterials 31*, 7386−7397.
(34) Vinogradov, S., and Wei, X. (2012) Cancer stem cells and drug resistance: the potential of nanomedicine. *Nanomedicine (London, U.K.) 7*, 597−615.
(35) Desai, M. P., Labhasetwar, V., Amidon, G. L., and Levy, R. J. (1996) Gastrointestinal uptake of biodegradable microparticles: effect of particle size. *Pharm. Res. 13*, 1838−1845.
(36) Wichitnithad, W., Nimmannit, U., Callery, P. S., and Rojsitthisak, P. (2011) Effects of different carboxylic ester spacers on chemical stability, release characteristics, and anticancer activity of mono-PEGylated curcumin conjugates. *J. Pharm. Sci. 100* (12), 5206−5218.
(37) Leu, B. L., and Huang, J. D. (1995) Inhibition of intestinal P-glycoprotein and effects on etoposide absorption. *Cancer Chemother. Pharmacol. 35* (5), 432−436.